ISSN: 0974-2115
www.jchps.com Journal of Chemical and Pharmaceutical Sciences

Computational Study on Surface pressure distribution and base pressure distribution over parabolic series nose cone

Harish S*, D. Hasen, V. Giridharan
Department of Aeronautical Engineering, Bharath institute of higher education and research, Selaiyur, Chennai, India
***Corresponding author:E-Mail:harishmit09@gmail.com**

ABSTRACT

This paper reports the computational results of surface pressure distribution, base pressure distribution and force coefficients of subsonic flow over parabolic nose cone series. Four parabolic series profile, of ¼ parabola, ½ parabola, ¾ parabola & full parabola, with same fineness ratio of 2.75 is used in this study. The computational analysis of flow over the four profiles is carried by ANSYS ICEM CF 15.0. Shear stress transport k-ω turbulence model was used for simulation. Flow domain was created with 5349604 tetrahedron elements. ANSYS CFX 15.0, commercially available software was used for preprocessing and post processing of the model. Results of surface pressure coefficient, base pressure coefficient and drag coefficient of the four parabolic series is presented. Full parabolic profile gives low surface pressure coefficient and high base pressure compared to other parabolic profiles. Hence the total drag coefficient over full parabolic profile is less compared the other profiles.

KEY WORDS: Parabolic nose cone; surface pressure distribution; base pressure; drag coefficient

1. INTRODUCTION

The Nose cone is forward most section of a rocket, guided missile or aircraft. Any object moving throught a fluid will experience a resistance and this resistance is directly proportional to the velocity of the moving object, shape of the object, properties of the fluid through which the object is moving. The resistance acting on the object in the direction of free stream velocity is called drag force. Aerodynamic design problem of any is concerned to determine the shape of the object which is having minimum drag coefficient C_d. In application like airplane, rocket or missile, or automobile it is required it reduce the drag, in some application, like parachute drag is beneficial factor. In rocket, missile or aircraft, forward most body is cone shape. There are many different nose cone shapes. There is other nose cone shape such as elliptical, ogive, Parabolic series in which profile is tangent to base. In the elliptical and ogive shape have blunt nose and but parabolic series has sharp nose. Study on surface pressure distribution and over parabolic series cone is discussed in this paper. Study was carried computationally using commercial available ANSYS ICEM CFD.

Computation:

Geometry and flow domain: Data point for the four parabolic series nose cone generated using the following equation

$$Y = R\left(\frac{\left(2x/L\right) - K(\frac{x}{L})^2}{2 - K}\right)$$

K = 0.25 for a ¼ parabola
K= 0.5 for a ½ parabola
K = 0.75 for ¾ parabola
K = 1 for a parabola

Nose cone has length of 110 mm and base diameter of 40 mm. Since the geometry is symmetrical is about vertical plane only of half of geometry is generated using the above data points, in order to reduce the computational load and time.

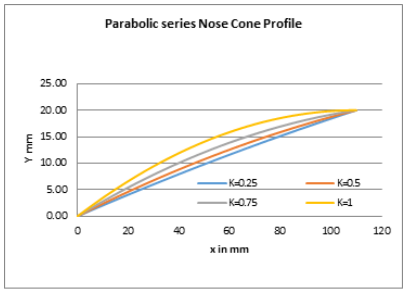

Fig.1. Parabolic series nose cone data points

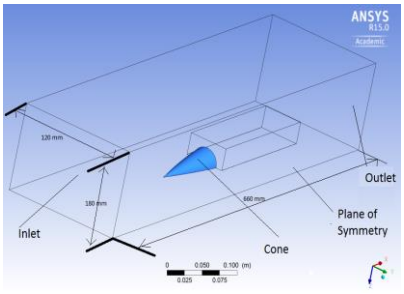

Fig.2. Computational Domain

The fineness ratio (L/D) for all profile is kept constant of 2.75. The computational domain consists of two domains model domain and wake domain as shown in fig 2. Model domain has dimension of 600 X 120 X 180 mm. A wake domain is created behind the nose cone. The wake domain captures with closely packed elements which is used to captures the recirculation zone and flow reattachment point behind the nose cone. Air is used as flow material.

Boundary condition: Inlet condition for the domain is given as velocity inlet with flow velocity of 80 m/s and output condition is taken as pressure outlet and bottom of domain is taken as symmetric and remaining side of the domain is taken as wall with no slip condition and adiabatic as shown in fig.2. Reference pressure for all computation is taken as 101210 Pa.

Solver: A finite volume coupled flow solver ANSYS – CFX 15 was used for the computation. The computational grid generated from ANSYS- ICEM CFD 15.0 was used for solving the flow equation. Three conservation equation such as continuity equation, energy equation, momentum equations in three direction (U-mom, v-Mom, w-mom) and turbulence equation for kinetic energy and eddy frequency were solved by the solver. Shear stress transport turbulence model is used for this study. Residual target of 1 x 10^{-4} was used as convergent criteria.

2. RESULT & DISCUSSION

Surface pressure coefficient: Comparison of computational results for four parabolic series nose cones are discussed here, Contour plots of absolute pressure distribution for the ¼ , ½ , ¾ and full parabolic profile is shown in fig 3, fig 4 , fig 5 fig 6 respectively. Fig 7 shows variation of surface pressure coefficient along the length of cone for the four parabolic series profile. Horizontal axis is defined as distance measured from tip of nose cone to base and vertical axis defined by pressure coefficient. The surface pressure coefficient decreases continuously from the nose tip to base region for all four profiles as shown in fig 3. Surface pressure distribution for full parabolic series nose has better surface distribution compared to other profile shape. As full parabolic shape have base tangent to profile hence flow leaves at base smooth and parallel to the free stream velocity direction. But in other profile the flow always leaves at certain angle to initial flow direction. Hence the pressure coefficient near the base is function of slope of the curve at base.

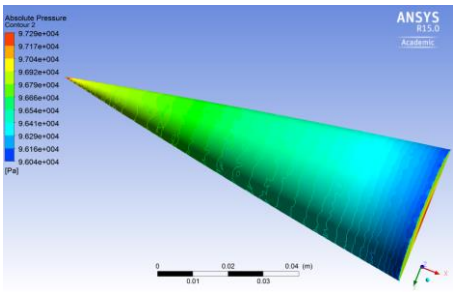

Fig.3. Contour of surface pressure for K = 0.25

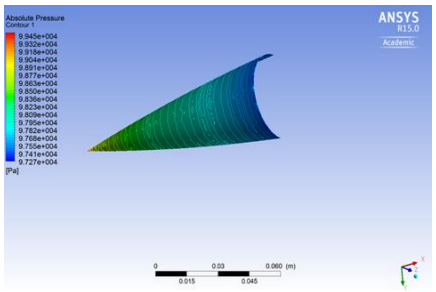

Fig.4. Contour of surface pressure for K = 0. 5

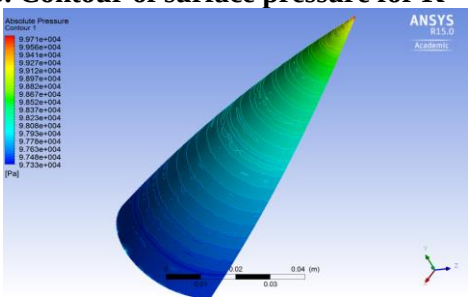

Fig.5. Contour of surface pressure for K = 0. 75

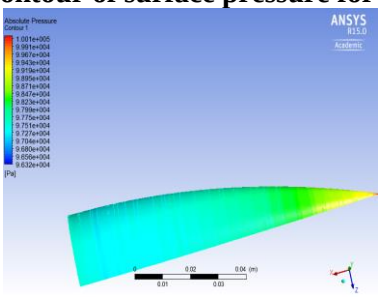

Fig.6. Contour of surface pressure for K = 1

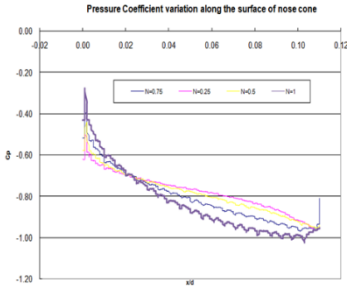

Fig.7. Surface pressure coefficient

Base Pressure Coefficient: Contour plots of base pressure distribution for the ¼ , ½ , ¾ and full parabolic profile is shown in fig 8, fig 9, fig 10 fig 11 respectively. Base pressure coefficient of four parabolic series is shown in fig 12. Horizontal axis shows the distance of one end of cone to other is measured in symmetric plane. Vertical axis shows the pressure coefficient. Fig 4 shows that full parabolic nose cone has increased base pressure and nearly all the pressure is recovered at center of base compared to other profiles.

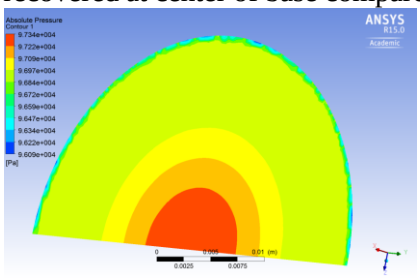

Fig.9. Base pressure contour for K = 0.5

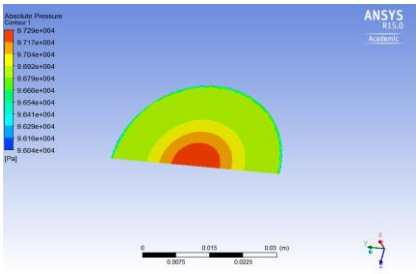

Fig.8. Base pressure contour for K = 0.25

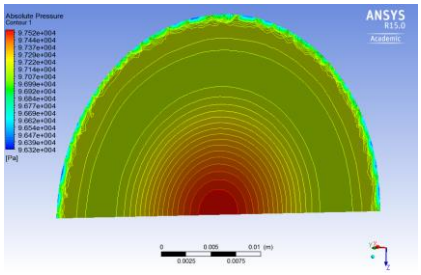

Fig.11. Base pressure contour for K = 1

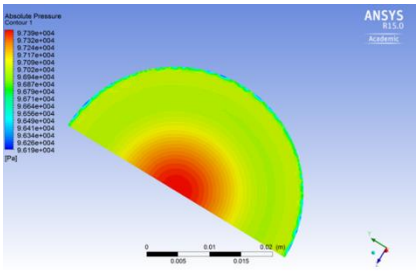

Fig.10. Base pressure contour for K = 0.75

Drag coefficeint Coefficient: Figure 13 show variation of drag coefficient due change in profile shape of parabolic series nose cone. From the fig 13 the drag coefficient decreases with increase in K. For full parabolic drag coefficient is low. This is due the surface pressure coefficient is lower for full parabolic nose is lower, and at the same time the base pressure coefficient for full parabolic nose is cone hence the net effect reduced drag coefficient for full parabolic series cone compared to other profile.

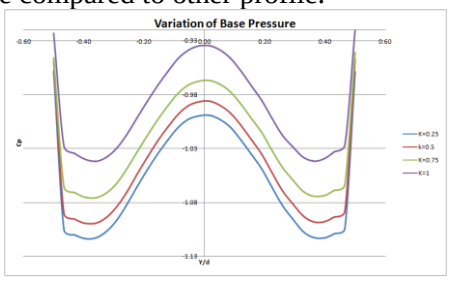

Fig.12. Base pressure coefficient

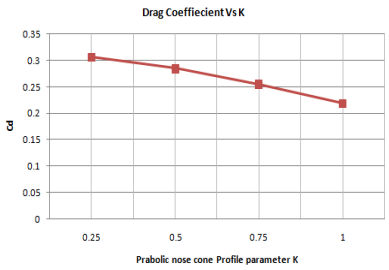

Fig.13. Base pressure coefficient

3. CONCULSIONS

Effect nose shape on surface pressure coefficient, base pressure coefficient and drag coefficient was discussed. The full parabolic nose cone has better surface pressure distribution and base pressure distribution compared to other parabolic series nose cone. It is found that drag coefficient for full parabolic series cone has less drag coefficient.

REFERENCES

Abdollah shadram, mahdi azimi fard and Noorallah Rostamy Experimental study of near wake flow behind rectangular cylinde, American Journal of applied science, 5 (8), 2008, 917-926.

Davis RW, Moor EF, Purtell LP, A Numerical- Experimental study of confined flow around rectangular cylindersm Physics Fluids, 27 (1), 1984, 46-59.

Gopalakrishnan K, Sundar Raj M, Saravanan T, Multilevel inverter topologies for high-power applications, Middle - East Journal of Scientific Research, 20 (12), 2014, 1950-1956.

Jasmin M, Vigneshwaran T, Beulah Hemalatha S, Design of power aware on chip embedded memory based FSM encoding in FPGA, International Journal of Applied Engineering Research, 10 (2), 2015, 4487-4496.

Kanniga E, Selvaramarathnam K, Sundararajan M, Kandigital bike operating system, Middle - East Journal of Scientific Research, 20 (6), 2014, 685-688.

Kanniga E, Sundararajan M, Modelling and characterization of DCO using pass transistors, Lecture Notes in Electrical Engineering, 86 (1), 2011, 451-457.

Karthik B, Arulselvi, Noise removal using mixtures of projected gaussian scale mixtures, Middle - East Journal of Scientific Research, 20 (12), 2014, 2335-2340.

Karthik B, Arulselvi, Selvaraj A, Test data compression architecture for lowpower vlsi testing, Middle - East Journal of Scientific Research, 20 (12), 2014, 2331-2334.

Karthik B, Kiran Kumar TVU, Authentication verification and remote digital signing based on embedded arm (LPC2378) platform, Middle - East Journal of Scientific Research, 20 (12), 2014, 2341-2345.

Karthik B, Kiran Kumar TVU, EMI developed test methodologies for short duration noises, Indian Journal of Science and Technology, 6 (5), 2013, 4615-4619.

Karthik B, Kiran Kumar TVU, Vijayaragavan P, Bharath Kumaran, E., Design of a digital PLL using 0.35Î¼m CMOS technology, Middle - East Journal of Scientific Research, 18 (12), 2013, 1803-1806.

Philomina S, Karthik B, Wi-Fi energy meter implementation using embedded linux in ARM 9, Middle - East Journal of Scientific Research, 20 (12), 2014, 2434-2438.

Saha AK, Muralidhar K, Biswas G. Experimental study of flow past a square cylinder at high Reynolds number. Experiments in fluids, 29, 2000, 553-563.

Saravanan T, Sundar Raj M, Gopalakrishnan K, Comparative performance evaluation of some fuzzy and classical edge operators, Middle - East Journal of Scientific Research, 20 (12), 2014, 2633-2633.

Saravanan T, Sundar Raj M, Gopalakrishnan K, SMES technology, SMES and facts system, applications, advantages and technical limitations, Middle - East Journal of Scientific Research, 20 (11), 2014, 1353-1358.

Sundararaj M, Sridhar B T N, Surface pressure study of elliptic cones at low speed. IETECH journal of Mechanical Design, 3 (2), 2009, 58-63.

Vijayaragavan SP, Karthik B, Kiran Kumar TVU, Privacy conscious screening framework for frequently moving objects, Middle - East Journal of Scientific Research, 20 (8), 2014, 1000-1005.

Vijayaragavan SP, Karthik B, Kiran Kumar TVU, A DFIG based wind generation system with unbalanced stator and grid condition, Middle - East Journal of Scientific Research, 20 (8), 2014, 913-917.

Vijayaragavan SP, Karthik B, Kiran Kumar TVU, Effective routing technique based on decision logic for open faults in fpgas interconnects, Middle - East Journal of Scientific Research, 20 (7), 2014, 808-811.